Acta Cryst. (1953). **6**, 543

The Interpretation of Diffuse X-ray Reflexions from Single Crystals. II

BY J. HOERNI* AND W. A. WOOSTER

Crystallographic Laboratory, Cavendish Laboratory, Cambridge, England

(*Received* 5 *December* 1952)

An earlier paper by the same authors dealt with geometrical aspects of the photographic study of diffuse X-ray reflexions from single crystals. The present paper deals with factors affecting the intensity of these reflexions. The method of making the observations varies according to whether the diffusely-scattering reciprocal region has the form of a cloud, a disc, a rod or a point, and the appropriate method for each is indicated. Divergence corrections are described which make allowance for the fact that the beam is not infinitely narrow and the crystal is not ideally perfect. The final intensity correction applies to reflexions which occur off the equator of the photograph.

X-ray diffuse reflexions may be referred to extensions of the reciprocal-lattice points caused by the lack of a truly periodic arrangement of the atoms in the crystal. In a previous paper (I) (Hoerni & Wooster, 1952), a method of relating any given point within the diffuse spot on a photograph to the corresponding point in reciprocal space has been described. The present paper deals with some aspects of intensity measurements of the diffuse reflexions. In particular, we shall discuss the influence of the distribution of the extra scattering density in reciprocal space on intensity measurements and the correction affecting the non-equatorial diffuse reflexions recorded with a cylindrical camera.

1. Intensity measurements which are necessary for the study of reciprocal clouds, discs, spikes and points

The diffuse scattering densities in reciprocal space may have four essentially different shapes, namely: (i) broad three-dimensional extensions or clouds; (ii) discs; (iii) spikes (rods); (iv) points.

These discs, spikes and points cannot be considered as infinitely narrow or sharp, owing to the finite size of the crystal. In order to write suitable expressions for their scattering power, we shall assume that the crystal is a parallelepiped with edges $N_1\mathbf{a}_1$, $N_2\mathbf{a}_2$ and $N_3\mathbf{a}_3$, where the $\mathbf{a}_i$'s stand for the unit-cell vectors, and the N's are large numbers. For convenience in calculations, the $\mathbf{a}_i$'s will be supposed to be orthogonal, but our results will also apply to non-orthogonal cases. If absorption in the crystal is neglected, the diffuse intensity for the four types of scattering densities can be written as follows:

$$\text{(i)} \quad I(\mathbf{b}) = (I_e/r^2)N_1N_2N_3g_{123}(\mathbf{b}) , \tag{1}$$

$$\text{(ii)} \quad I(\mathbf{b}) = (I_e/r^2)N_2N_3G(\mathbf{b}_1)g_{23}(\mathbf{b}_2, \mathbf{b}_3) \quad \text{for a disc normal to } \mathbf{a}_1 , \tag{2}$$

$$\text{(iii)} \quad I(\mathbf{b}) = (I_e/r^2)N_1G(\mathbf{b}_2)G(\mathbf{b}_3)g_1(\mathbf{b}_1) \quad \text{for a spike parallel to } \mathbf{a}_1 , \tag{3}$$

$$\text{(iv)} \quad I(\mathbf{b}) = (I_e/r^2)G(\mathbf{b}_1)G(\mathbf{b}_2)G(\mathbf{b}_3)g . \tag{4}$$

In the above expressions

$\mathbf{b} = (\mathbf{b}_1, \mathbf{b}_2, \mathbf{b}_3)$, denotes the reciprocal point corresponding to the direction of observation;

$I_e = I_0(e^2/mc^2)^2 . \frac{1}{2}(1+\cos^2 2\theta)$, represents the intensity scattered by a free electron at unit distance from the crystal, when irradiated with unpolarized radiation of intensity I_0, the angle of scattering being 2θ;

r = distance from the crystal at which the diffuse intensity is measured;

g is a constant (depending on the atomic arrangement);

g_1, g_{23}, g_{123} are functions which vary slowly with $\mathbf{b}$;

$G(\mathbf{b}_i) = (\sin^2 \pi N_i\mathbf{a}_i\mathbf{b})/(\sin^2 \pi\mathbf{a}_i\mathbf{b})$ and has a maximum value N_i^2 when $\mathbf{a}_i\mathbf{b}$ takes integral values and falls to zero when $\mathbf{a}_i\mathbf{b}$ is increased by the small amount $1/N_i^2$.

The function $G(\mathbf{b}_i)$ varies so rapidly that the following factors entirely mask its variation: (*a*) the incident beam is not strictly parallel; (*b*) the solid angle subtended by the crystal, at the distance where the diffuse intensity is observed, is not vanishingly small; (*c*) the recording instruments, namely the microphotometer or the Geiger counter, do not cover a vanishingly small section of the diffuse beam. Consequently, the intensity $\bar{I}(\mathbf{b})$, say, measured by means of a photographic film or a Geiger counter, may be different from the theoretical expressions (1)–(4). Any measurement $\bar{I}(\mathbf{b}^0)$ relating to a reciprocal point $\mathbf{b}^0$ records the contributions of the reciprocal points contained in the 'divergence domain' $\Delta(\mathbf{b}^0)$, the dimensions of which are small relative to those of the re-

* Present address: California Institute of Technology, Pasadena, California, U.S.A.

ciprocal unit cell, but large compared with the distances over which the functions $G(\mathbf{b}_i)$ differ from zero. Every point within $\Delta(\mathbf{b}^0)$ does not contribute equally to the recorded intensity $\bar{I}(\mathbf{b}^0)$. Its contribution is weighted by the divergence function $h(\mathbf{b}-\mathbf{b}^0)$, which vanishes outside $\Delta(\mathbf{b}^0)$ and within $\Delta(\mathbf{b}^0)$ depends on the experimental conditions. The observed intensity $\bar{I}$ is therefore related to the true intensity I by the formula

$$\bar{I}(\mathbf{b}^0) = \int_{\Delta} I(\mathbf{b})h(\mathbf{b}-\mathbf{b}^0)dv_b\,, \qquad (5)$$

where h is normalized by writing

$$\int_{\Delta} h(\mathbf{b}-\mathbf{b}^0)dv_b = 1\,.$$

We shall now study the divergence effects for the four types of scattering densities by substituting in turn (1), (2), (3) and (4) in (5).

Case (i)

Assuming that the variation of $g_{123}(\mathbf{b})$ over $\Delta(\mathbf{b}^0)$ is negligible, we obtain

$$\bar{I}(\mathbf{b}^0) = \frac{I_e}{r^2}N_1N_2N_3g_{123}(\mathbf{b}^0)\int h(\mathbf{b}-\mathbf{b}^0)dv_b$$
$$= \frac{I_e}{r^2}N_1N_2N_3g_{123}(\mathbf{b}^0) = I(\mathbf{b}^0)\,. \qquad (6)$$

Thus, intensity measurements are not affected in this case by the divergence function h, and I is proportional to the function g_{123}.

Case (ii)

To a first approximation, the divergence function h can be expressed as the product of three one-variable functions h_1, h_2, h_3, each normalised in the same way as h, namely,

$$h(\mathbf{b}-\mathbf{b}^0) = h_1(\mathbf{b}_1-\mathbf{b}_1^0)h_2(\mathbf{b}_2-\mathbf{b}_2^0)h_3(\mathbf{b}_3-\mathbf{b}_3^0)\,. \qquad (7)$$

Substitution of (2) and (7) in (5) gives, then,

$$\bar{I}(\mathbf{b}^0) = \frac{I_e}{r^2}N_2N_3\int G(\mathbf{b}_1)h_1(\mathbf{b}_1-\mathbf{b}_1^0)d\mathbf{b}_1$$
$$\times\int\int g_{23}(\mathbf{b}_2,\mathbf{b}_3)h_2(\mathbf{b}_2-\mathbf{b}_2^0)h_3(\mathbf{b}_3-\mathbf{b}_3^0)d\mathbf{b}_2d\mathbf{b}_3$$
$$= \frac{I_e}{r^2}N_2N_3\bar{G}(\mathbf{b}_1^0)g_{23}(\mathbf{b}_2^0,\mathbf{b}_3^0)\,, \qquad (8)$$

since g_{23} varies slowly. The function $\bar{G}(\mathbf{b}_1^0)$ is given by the equation

$$\bar{G}(\mathbf{b}_1^0) = \int G(\mathbf{b}_1)h_1(\mathbf{b}_1-\mathbf{b}_1^0)d\mathbf{b}_1\,,$$

and it is very different from $G(\mathbf{b}_1)$, as may be seen in Fig. 1, where the function h, G and $\bar{G}$ are shown. A streak, corresponding to the intersection of the Ewald sphere, Σ, (Fig. 2) by a disc, may be observed, but none of the observed intensities $\bar{I}$ is related in a simple way to the true intensity I. However, we shall show that the quantity which it is most useful to measure is $I_l = \int \bar{I}dl$, namely, the observed intensity integrated along a straight line crossing the streak

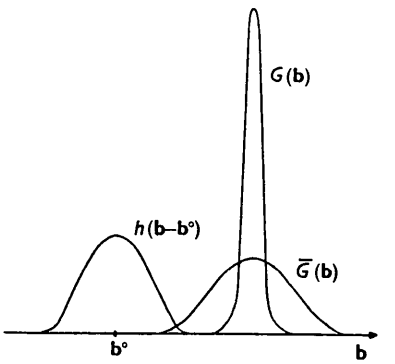

Fig. 1. Diagram showing the divergence function $h(\mathbf{b}-\mathbf{b}^0)$ (for a reflexion about a mean position $\mathbf{b}^0$), a function $G(\mathbf{b})$ giving the true variation of diffraction about a position $\mathbf{b}$, and $\bar{G}(\mathbf{b})$ giving the observed variation of diffraction about the same position. (The curve for $h(\mathbf{b}-\mathbf{b}^0)$ has been arbitrarily placed along the axis of abscissae.)

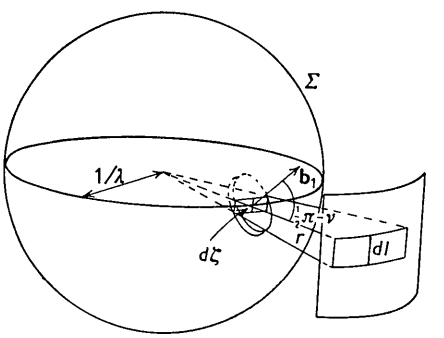

Fig. 2. Diagram showing the intersection of a reciprocal disc with the Ewald sphere, and the projection of the surface of intersection on to the photographic film.

orthogonally. It is easy to see (Fig. 2) that dl, the breadth of the photographic streak, corresponds to a reciprocal distance $d\zeta = dl/r\lambda$ on the surface of the Ewald sphere (of radius $1/\lambda$). Furthermore, if the normal to the disc makes an angle $(\frac{1}{2}\pi-\nu)$ with the radius of the sphere, $d\zeta = d\mathbf{b}_1/\cos\nu$, or $dl = (r\lambda/\cos\nu)d\mathbf{b}_1$.

Applying this to equation (8) we obtain

$$\int \bar{I}dl = \frac{I_e\lambda}{r}\frac{1}{\cos\nu}N_2N_3g_{23}(\mathbf{b}_2^0,\mathbf{b}_3^0)\int \bar{G}(\mathbf{b}_1^0)d\mathbf{b}_1^0\,. \qquad (9)$$

But

$$\int \bar{G}(\mathbf{b}_1^0)d\mathbf{b}_1^0 = \int\left(\int G(\mathbf{b}_1^0)h(\mathbf{b}_1-\mathbf{b}_1^0)d\mathbf{b}_1^0\right)d\mathbf{b}_1$$
$$= \int G(\mathbf{b}_1)d\mathbf{b}_1\int h(\mathbf{b}_1-\mathbf{b}_1^0)d\mathbf{b}_1 = \int G(\mathbf{b}_1)d\mathbf{b}_1 = \frac{N_1}{\mathbf{a}_1};$$

that is to say the areas under curves G and $\bar{G}$ in Fig. 1 have the same value, namely, $N_1/\mathbf{a}_1$. Equation (9) then becomes, dropping the superscript 0,

$$\int \bar{I} dl = \frac{I_e \lambda}{r} \frac{1}{\cos \nu} N_1 N_3 N_3 \frac{1}{\mathbf{a}_1} g_{23}(\mathbf{b}_2, \mathbf{b}_3) . \quad (10)$$

Thus, the integral across the streak is proportional to the function g_{23} for the density of the disc multiplied by the factor $1/\cos \nu$. This can also be seen in a simple geometrical manner from Fig. 2, where the integration of blackening along dl can be seen to give a representative measure of the total scattering power across the disc.

Case (iii)

Calculations similar to those used in studying case (ii) can be made here. A sharp spot corresponding to the intersection with the Ewald sphere of the spike is observed, and the relevant experimental quantity is now $\int \bar{I} dS$, namely, the observed intensity integrated over the whole spot. To an area dS on the film there corresponds on the reflecting sphere an area $d\sigma = dS/r^2\lambda^2$ (Fig. 3) and if the angle between the spike

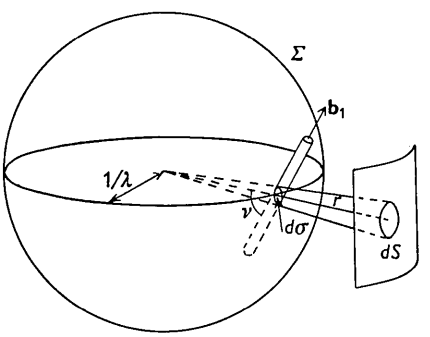

Fig. 3. Diagram showing the intersection of a reciprocal spike with the Ewald sphere and the projection of the surface of intersection on to the photographic film.

and the radius of the sphere is ν, $d\sigma = d\mathbf{b}_2 d\mathbf{b}_3/\cos \nu$. The integral $\int \bar{I} dS$ becomes, using (3), (5) and (7),

$$\int \bar{I} dS = I_e \lambda^2 \frac{1}{\cos \nu} N_1 g_1(\mathbf{b}_1) \int\int \bar{G}(\mathbf{b}_2) \bar{G}(\mathbf{b}_3) d\mathbf{b}_2 d\mathbf{b}_3$$
$$= I_e \lambda^2 \frac{1}{\cos \nu} N_1 N_2 N_3 \frac{1}{\mathbf{a}_2 \mathbf{a}_3} g_1(\mathbf{b}_1) . \quad (11)$$

The integral over the spot is therefore proportional to the function g_1 for the density of the spike multiplied by the factor $1/\cos \nu$. It may also be seen from Fig. 3 that the intensity integrated over the whole spot on the film gives a measure of the density of the reciprocal spike across a particular section.

Case (iv)

The diffraction from reciprocal points includes, in particular, the usual Bragg reflexion which corresponds to the passage through the Ewald sphere of the reciprocal lattice points themselves. The relevant experimental quantity is here the 'integrated reflexion' $E\omega/I_0$, where E is the total energy diffracted when the point is rotated with an angular velocity ω across the Ewald sphere. Using the notation of this paper, the integrated reflexion is expressed by

$$\frac{E\omega}{I_0} = \frac{I_e \lambda^3}{I_0} \frac{1}{\xi \cos \nu} N_1 N_2 N_3 \frac{1}{\mathbf{a}_1 \mathbf{a}_2 \mathbf{a}_3} g , \quad (12)$$

where ξ/λ is the rotation radius of the point. For a point lying in the equatorial plane of a cylindrical camera $\xi = 2 \sin \theta$ and $\nu = \theta$ so that (12) takes the more familiar form

$$\frac{E\omega}{I_0} = \frac{I_e \lambda^3}{I_0} \frac{1}{\sin 2\theta} \left(\frac{1}{\mathbf{a}_1 \mathbf{a}_2 \mathbf{a}_3} \right)^2 g V , \quad (13)$$

where V is the volume of the crystal and g, for the particular case of a Bragg reflexion, is equal to the square of the structure amplitude.

The factor $1/\xi \cos \nu$ in (12)—or $1/\sin 2\theta$ in (13)—is the Lorentz factor. It will be seen that the factors $1/\cos \nu$ in (10), (11) and (12) arise from the same cause, namely, the inclination of the disc or of the spike relative to the Ewald sphere. For this reason, it is suggested that $1/\cos \nu$ should be called the 'Lorentz factor for diffuse reflexions'.

2. Divergence corrections

The above formulae (6), (10) and (11) are strictly valid only on the assumption that the variations of the function $g(\mathbf{b})$—where $g(\mathbf{b})$ is any one of the functions $g_1(\mathbf{b}_1)$, $g_{23}(\mathbf{b}_2 \mathbf{b}_3)$, $g_{123}(\mathbf{b}_1, \mathbf{b}_2, \mathbf{b}_3)$—over the divergence domain $\Delta(\mathbf{b})$ can be neglected. This is often the case in actual experiments, especially when the diffuse reflexions are recorded photographically since the divergence effect (c) is then smaller than in the case of a Geiger counter. Divergence corrections do not arise for Bragg reflexions, since g in (4) is a constant. On the other hand, when

$$\bar{g}(\mathbf{b}^0) = \int g(\mathbf{b}) h(\mathbf{b} - \mathbf{b}^0) dv_b$$

happens to be different from $g(\mathbf{b}^0)$ the explicit form of h has to be determined experimentally. Then the passage from the observed function $\bar{g}(\mathbf{b})$ to the true function $g(\mathbf{b})$ can be made as follows:

A new integral

$$\bar{\bar{g}}(\mathbf{b}^0) = \int \bar{g}(\mathbf{b}) h(\mathbf{b} - \mathbf{b}^0) dv_b$$

is calculated from the observed values $\bar{g}(\mathbf{b})$ corresponding to the various points within Δ. Since the divergence correction is usually small, it can be assumed that the effect of h on g and $\bar{g}$ is the same, or in other words that the following relation holds, namely,

$$\frac{\bar{\bar{g}}(\mathbf{b}^0)}{\bar{g}(\mathbf{b}^0)} = \frac{\bar{g}(\mathbf{b}^0)}{g(\mathbf{b}^0)} ,$$

from which the true value $g(\mathbf{b}^0)$ can be obtained.

Practical applications of the above method of calculating divergence corrections can be found in studies of diffuse reflexions by Olmer (1948), Ramachandran (1949) and Hoerni (1952).

3. The inclination factor for non-equatorial spots

We now come to further factors affecting intensity measurements in the case of non-equatorial diffuse spots recorded with a cylindric camera. These factors are due to: (*A*) the increased quantity of photographic emulsion bathed in a given X-ray beam at oblique incidence; (*B*) the increased absorption of X-rays in the film at oblique incidence; (*C*) the increased distance between the crystal and the point where X-rays are recorded.

According to the considerations of § 1, we must investigate the effect of factors A, B and C in the case of the different spots arising from the four types (i)–(iv) of scattering densities in reciprocal space. We have already found that the relevant experimental quantities are: (1) the intensity I at a given point within the diffuse spot; (2) the line integral $I_l = \int I dl$ along a given normal section of a spike; (3) the surface integral or flux $J = \int I dS$ over a sharp spot. We have therefore to consider the effect of factors A, B and C on each of the quantities (1), (2) and (3).

Factor A

For convenience, we shall deal with a beam of constant intensity I and of cross-section S. If the beam is allowed, in the first instance, to fall normally on the film, the value I is deduced from microphotometer measurements, while the flux is equal to $J = IS$. Clearly, the flux is proportional to the quantity of photographic emulsion bathed in the beam so that this quantity is multiplied by the factor $\sec\chi$ when the beam is allowed to fall on the film at an angle χ with the normal to the film. While the new flux J' is thus equal to $J\sec\chi$, the measurements for I are not affected since $I' = J'/S\sec\chi = J\sec\chi/S\sec\chi = I$. As regards the line integral I_l, the effect of factor A depends on the angle (measured on the film) between the direction of integration and the equatorial direction. We have $I_l' = \int I' dl' = \int I dl'$, since $I = I'$, so that the relation between I_l' and I_l depends on the way in which the length element dl is modified by rotating the film by an angle χ about the equatorial direction. Clearly, dl is not affected when the direction of integration is parallel to the equatorial direction (i.e. in the case of a spike normal to the equatorial direction) whereas $dl' = dl\sec\chi$ when the direction of integration is vertical (i.e. in the case of a spike, parallel to the equatorial line). For a general direction, it may be shown that $dl' = dl(1-\sin^2\chi.\sin^2\alpha)^{-\frac{1}{2}}$, where α is the angle between the direction of integration and the equatorial direction.

Factor B

This factor is related to the increased absorption of X-rays at oblique incidence. It affects only the factor I in I_l and J, and is therefore the same for the quantities (1), (2) and (3). The ratio between the intensity at normal incidence I and the intensity at oblique incidence I' has been found by Cox & Shaw (1930) to be equal to

$$I/I' = [1+\exp[-\mu t](1-C)]/[1+\exp[-\mu t\sec\chi](1-C\sec\chi)],$$

where t and μ are the thickness and the absorption coefficient of the celluloid backing of the film, and C is the loss of intensity from the beam in the front layer of emulsion at normal incidence. These authors also give the experimental way of determining the constants (μt) and C.

According to (6), (9) and (10), I and I_l are proportional to $1/r^2$ and $1/r$ respectively, whereas J does not depend on the distance r from the crystal. Hence, if the camera radius is taken as the standard distance

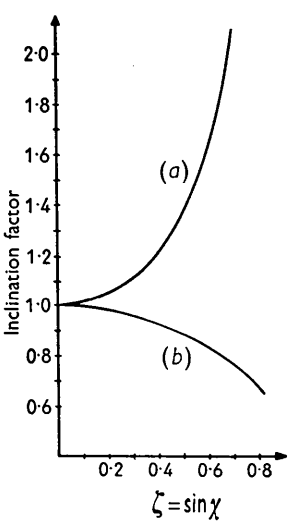

Fig. 4. Graph showing the variation of the *inclination factor* with ζ for the intensity at a point on the film (curve (*a*)), and for the integrated intensity over an area (curve (*b*)).

Table 1. *Inclination factor for non-equatorial spots*

Experimental quantity	Factor A	Factor B	Factor C
I	1	$\dfrac{1+\exp[-\mu t](1-C)}{1+\exp[-\mu t\sec\chi](1-C\sec\chi)}$	$\sec^2\chi$
$I_l = \int I dl$	$(1-\sin^2\chi\sin^2\alpha)^{\frac{1}{2}}$		$\sec\chi$
$J = \int I dS$	$\cos\chi$		1

of observation, the values of I, I_l and J found for non-equatorial diffuse spots must be multiplied by $\sec^2 \chi$, $\sec \chi$ and 1 respectively.

Table 1 summarizes the values found for the partial inclination factors by which the observed quantities I', I_l' and J' are to be multiplied. The total inclination factor is obtained by multiplying the three factors along the appropriate horizontal line.

The total factor for J is similar to the 'film-absorption factor' found by Cox & Shaw (1930) in their study of integrated reflexion. It is plotted in Fig. 4 (curve (*b*)) as a function of $\zeta = \sin \chi$, using Cox & Shaw's experimental values for C and (μt). In the same figure, the corresponding inclination factor for I has also been plotted (curve (*a*)).

One of us (J.H.) wishes gratefully to acknowledge the award of a scholarship by the Swiss Commission for Post Doctoral Studies in Mathematics and Physics.

References

Cox, E. G. & Shaw, W. F. B. (1930). *Proc. Roy. Soc.* A, **127**, 71.
Hoerni, J. (1952). Thesis, Cambridge.
Hoerni, J. & Wooster, W. A. (1952). *Acta Cryst.* **5**, 626.
Olmer, Ph. (1948). *Bull. Soc. Franç. Minér.* **71**, 145.
Ramachandran, G. N. (1949). Thesis, Cambridge.

Acta Cryst. (1953). **6**, 547

The Crystal and Molecular Structure of B_4Cl_4

By Masao Atoji and William N. Lipscomb

School of Chemistry, University of Minnesota, Minneapolis 14, *Minnesota, U.S.A.*

(*Received* 6 *December* 1952)

The molecule B_4Cl_4 consists of a nearly regular tetrahedron of boron atoms surrounded by a larger, nearly regular tetrahedron of chlorine atoms with B–Cl single bonds (1·70 Å) directed away from the center of the tetrahedra. The molecular symmetry is D_{2d}–$\bar{4}2m$, but differs only slightly from T_d–$\bar{4}3m$, and the average B–B distance is 1·70 Å. Molecular centers are at 0, 0, $\frac{1}{2}$ and $\frac{1}{2}$, $\frac{1}{2}$, 0 in the space group D_{4h}^{15}–$P4_2/nmc$, with $a = b = 8{\cdot}09$ Å and $c = 5{\cdot}45$ Å.

The unusual compound, B_4Cl_4, has recently been discovered by Urry, Wartik & Schlesinger (1952), who have kindly supplied us with a sample for molecular structure determination by the X-ray diffraction method. This study is part of a general program of structure determinations of electron deficient compounds of boron.

The sample was distilled carefully into thin-walled pyrex capillaries in a vacuum line previously flushed with BF_3 in order to remove reactive compounds adsorbed on the glass surfaces. The samples in these capillaries were stored about two weeks at about 35° C. with a small temperature gradient in the capillary in order to grow a single crystal about 0·3 by 0·5 by 1·2 mm. The symmetry of the tetragonal reciprocal lattice is D_{4h}–$4/mmm$. The unit-cell dimensions of

$$a = b = 8{\cdot}09 \pm 0{\cdot}02 \quad \text{and} \quad c = 5{\cdot}45 \pm 0{\cdot}01 \text{ Å}$$

lead to a unit cell volume of 356 Å^3. Assuming the usual values for van der Waals radii this unit cell must contain two molecules of B_4Cl_4, and the crystal therefore has the reasonable calculated density of 1·724 g.cm.$^{-3}$. Because of the reactivity of the compound no independently measured value is known.

Buerger precession photographs of the $\{0kl\}$, $\{hhl\}$, $\{h,2h,l\}$ and $\{h,3h,l\}$ zones, and Weissenberg photographs of the $\{hk0\}$ zone were taken with Mo $K\alpha$ radiation. Intensities were estimated visually with the aid of standard scales prepared by timed exposures of a reflection from the crystal, and timed exposures of the various zones or multiple-film techniques were employed as additional aids. The revised Lorentz factor (Waser, 1951) was used in the reduction of the intensities of the precession photographs. Systematic extinctions of hhl when l is odd and of $hk0$ when $h+k$ is odd lead uniquely to the space group D_{4h}^{15}–$P4_2/nmc$. The presence of only two molecules in this space group requires the molecular symmetry to be D_{2d}–$\bar{4}2m$.

Both packing considerations and the presence of fairly strong reflections which would be approximately extinguished by choice of positions 8(*e*) or 8(*f*) lead to the positions 8(*g*) (*Internationale Tabellen*, 1935, p. 222) for the chlorine atoms. The x and z parameters in these positions,

$$0, x, z;\ x, 0, \bar{z};\ \tfrac{1}{2}, \tfrac{1}{2}+x, \tfrac{1}{2}-z;\ \tfrac{1}{2}+x, \tfrac{1}{2}, \tfrac{1}{2}+z;$$
$$0, x, \bar{z};\ \bar{x}, 0, \bar{z};\ \tfrac{1}{2}, \tfrac{1}{2}-x, \tfrac{1}{2}-z;\ \tfrac{1}{2}-x, \tfrac{1}{2}, \tfrac{1}{2}+z,$$

were estimated by trial-and-error methods with the aid of charts described by Bragg & Lipson (1936). The electron-density projections along [001] and [100] were then synthesized with the use of signs evaluated from the chlorine contributions only. Although no assumption had been made of the boron positions, these atoms appeared on the electron-density maps in